

Multi-Turn Multi-Gap Transmission Line Resonators - First Tests at 7 T

Roberta Kriegl^{1,2}, Jean-Christophe Ginefri², Marie Poirier-Quinot², Zhoujian Li², Luc Darrasse², Ewald Moser^{1,3}, and Elmar Laistler^{1,3}

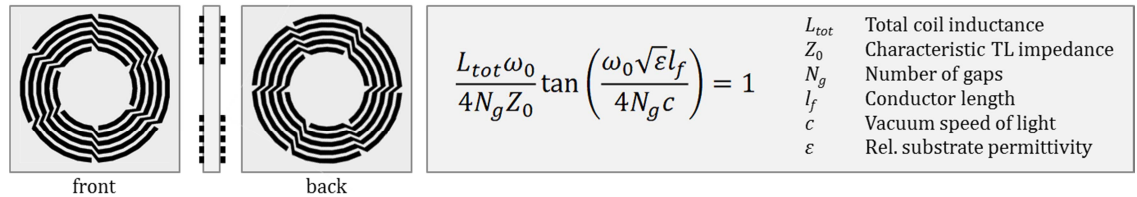
¹Center for Medical Physics and Biomedical Engineering, Medical University, Vienna, Vienna, Austria, ²IR4M (Imagerie par Résonance Magnétique Médicale et Multi-Modalités), UMR8081 CNRS, Université Paris Sud, Orsay, Essonne, France, ³MR Centre of Excellence, Medical University, Vienna, Vienna, Austria

Target audience: Researchers interested in RF engineering, form-fitting RF coils and their applications

Purpose: Self-resonant monolithic transmission line resonators (TLRs) [1,2] have been applied in numerous studies as highly sensitive miniaturized and/or superconducting surface probes. They consist of single- or multi-turn flat conductive windings, which are intersected by small gaps and deposited on both sides of a dielectric substrate. The use of flexible substrate materials enables form-fitting TLRs to various sample geometries, leading to a significant SNR gain [3]. So far, high-field applications requiring a FOV larger than a few square-centimeters could only be addressed by single-turn TLR technology with substantial limitations to optimize winding shape, current distribution, and B_1 pattern. The reason for this limitation is the intrinsically low resonance frequency of large multi-turn TLRs resulting from their high inductance. Here, a novel TLR design - the multi-turn multi-gap (MTMG) TLR [4] - is presented, which enables the use of large multi-turn TLRs at high static magnetic field strength.

Figure 1:

Example of a MTMG TLR (left). Front and back view as well as a crosssectional (not to scale) view are shown. Resonance condition for TLRs [1] (right).



Methods: The MTMG TLR design exploits the fact that the resonance frequency of a TLR increases almost linearly with the number of gaps. The resonance frequency can be deduced from the equation shown in Fig. 1, [1]. Up to now, TLRs with more than one gap per conducting band existed only in single-turn configuration because no design scheme for multiple turns was available. An example of the novel MTMG TLR design is shown in Fig. 1.

Three different MTMG-TLRs with an external diameter of 10 cm were designed for ^1H imaging at 7 T. The three coils are labeled 2T-5cm, 2T-8cm, and 5T-6cm according to their respective number of turns and their approximate inner diameter (1st column of Fig. 2). Note that such a coil size could not have been achieved for 300 MHz with the standard multi-turn TLR design. The MTMG-TLRs were fabricated on 790 μm thick PTFE (“Teflon”) substrate with standard photolithographic etching techniques by a third party (db electronic, Daniel Boeck SAS, Saint-Louis, France).

The performance of the MTMG TLRs was evaluated in FDTD simulations (XFDTD 7.3, Remcom, State College, PA, USA) combined with circuit co-simulation (ADS, Agilent, Santa Clara, USA), and MR measurements (Magnetom 7 T MRI, Siemens Medical Solutions, Erlangen, Germany). Post-processing of the simulation data was performed in Matlab (Mathworks, Natick, USA) using the SimOpTx toolbox (Medical University of Vienna, Vienna, Austria). The current density distribution in the front and back conductors, B_1^+ profiles normalized to 1 W input power, and 10g-averaged SAR values were simulated. In MRI experiments, flip angle maps employing the satTFL method [5] using a sinc-shaped slice-selective saturation pulse (2 ms pulse duration, 100 V reference amplitude) were acquired. The MTMG-TLRs were fine-tuned and matched inductively with a 5-cm pick-up loop placed at a distance of 4 cm above the TLRs; the coils were driven in transmit/receive mode.

Results: Simulation and B_1 mapping results are summarized in Fig. 2. The simulated current density distributions J (2nd column) show that the current is maximal at the center of the individual conductive strips forming the MTMG-TLRs and minimal at their respective ends. Maximum intensity projections (MIPs) of the simulated 10g-averaged SAR (3rd column) vary slightly in spatial distribution with the inner diameter of the investigated MTMG-TLRs. Further, it can be seen that the SAR values are highest for the 5T-6cm TLR. This might be related to the high density of turns or the high number of gaps for this design, and a higher current amplitude potentially resulting therefrom. The simulated B_1^+ profiles (4th column) show that the B_1 distribution varies strongly among the compared coil designs. While the 2T-5cm TLR produces a high B_1^+ over a narrow lateral FOV, the 2T-8cm TLR generates a lower B_1^+ but over a broader FOV; the B_1^+ profile of the 5T-6cm TLR appears to represent a compromise between the former two. The acquired flip angle maps (5th column) are in good qualitative agreement with simulation.

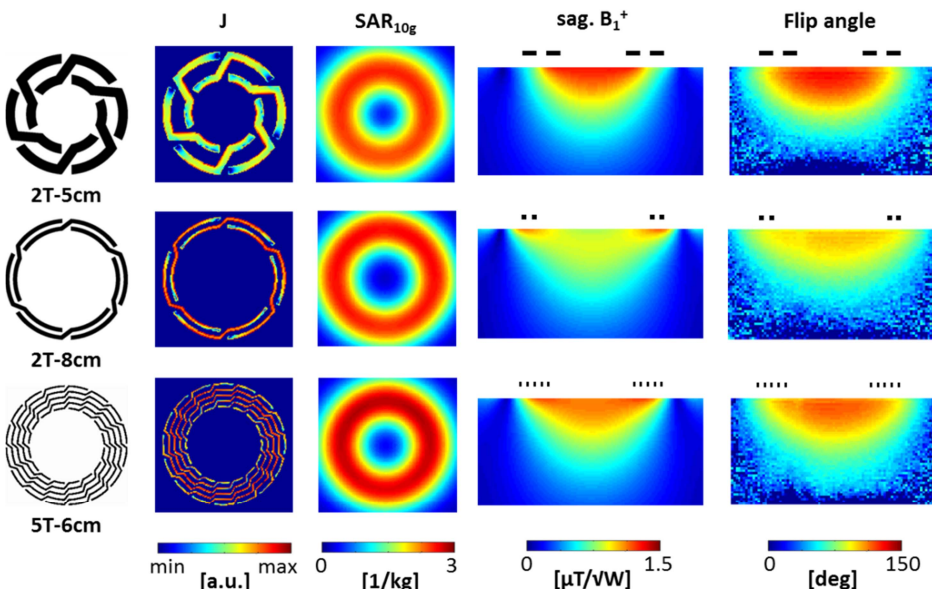


Figure 2:

1st column: The three investigated MTMG-TLR designs, only front conductor shown.

2T-5cm: conductor width $w = 6.8$ mm, spacing between turns $p = 10.7$ mm, number of gap $N_g = 6$

2T-8cm: $w = 3$ mm, $p = 3.3$ mm, $N_g = 6$

5T-6cm: $w = 1.5$ mm, $p = 3.1$ mm, $N_g = 16$

2nd column: Simulated current density distributions normalized to the maximum value, on a logarithmic scale

3rd column: Simulated SAR_{10g} MIPs

4th column: Simulated sagittal B_1^+ profiles

5th column: Measured flip angle distributions in a sagittal slice.

The distance between the TLRs and the phantom was 12 mm. The black bars above the B_1^+ profiles and the flip angle maps indicate the position of the conductors.

Conclusion: A novel design scheme for monolithic TLRs and its first application at 7 T is presented. Although the MTMG-TLR design is expected to benefit primarily biomedical ultra-high frequency MRI applications, it is applicable for any field strength or coil size. The additional degree of freedom in TLR design offered by the MTMG principle enables more efficient optimization of coil geometry, current distribution, and B_1 pattern, also for small low-frequency TLRs, and – due to its monolithic design – in principle also for thin-film superconducting coils.

References: [1] Gonord P et al., Magn Reson Med 1988; 6:353–358. [2] Serfaty S et al., Magn Reson Med 1997; 38:687–689. [3] Woytasik M et al., Microsyst Technol 2006; 13:1575–1580. [4] Kriegl R et al., Proc ESMRMB 2013. #441. [5] Chung S et al. Magn Reson Med 2010; 64:439–446.